remote sensing

MDPI

Article

Small Recreational Boat Detection Using Sentinel-1 Data for the Monitoring of Recreational Ecosystem Services

Marek Ruciński [1,2], Edyta Woźniak [1,*], Sylwia Kulczyk [2] and Marta Derek [2]

[1] Space Research Center, Polish Academy of Sciences, Bartycka 18a, 00-716 Warszawa, Poland
[2] Faculty of Geography and Regional Studies, University of Warsaw, Krakowskie Przedmieście 30, 00-927 Warszawa, Poland
* Correspondence: ewozniak@cbk.waw.pl; Tel.: +482-2496-6205

Abstract: Recreational ecosystem services are crucial for human well-being, and nature-based recreational activities often support local economies. However, tourism is very often one of many threads that contribute to the environment, and, therefore, data regarding its spatial patterns are necessary for the long-term sustainable development of a region. The present study describes a method for the detection of small boats (<10 m in length) in lake conditions based on Sentinel-1 radar images. Our two-step algorithm uses adaptive thresholding and math morphology operators to extract boat detections. The algorithm was validated on 14 images of different types of lakes in the Great Masurian Lake District, Poland. The detection accuracy was 88.17%. We also assessed the spatial and temporal distribution of tourist traffic and compared satellite data to field data. The correlation between the satellite-based map and field observations was 0.76.

Keywords: remote sensing; synthetic aperture radar; recreational boat detection; Sentinel-1; recreational ecosystem services

check for updates

Citation: Ruciński, M.; Woźniak, E.; Kulczyk, S.; Derek, M. Small Recreational Boat Detection Using Sentinel-1 Data for the Monitoring of Recreational Ecosystem Services. *Remote Sens.* **2023**, *15*, 1807. https://doi.org/10.3390/rs15071807

Academic Editor: Alessandra Budillon

Received: 23 December 2022
Revised: 2 March 2023
Accepted: 3 March 2023
Published: 28 March 2023

1. Introduction

Recreational boating is increasing globally, both at sea and on lakes [1,2]. While it is often an important element of the economy, and a driver of local and regional development, the growing interest in spending free time on water poses numerous management problems, both environmental and social. Quantitative data on boating traffic and its spatial diversity are crucial to inform policy decisions and support the sustainable management of water bodies [3], especially protected ones. These areas are usually the most vulnerable and, at the same time, the most popular among visitors [4,5]. Therefore, this article aims to develop a novel approach for monitoring boat traffic on lakes, using radar remote sensing. This method not only allows us to monitor spatial distribution of recreational boating in a lake district, but also to analyze its weekly and seasonal patterns, which is of a great importance for planning and management on the local and regional scales.

The absence of appropriate management schemes can result in a number of negative impacts.

Within a waterbody, pollution (e.g., due to septic tank discharge from boats [6]), the reduced abundance and structural complexity of aquatic vegetation [7], and the destabilization of the seabed due to anchoring [8] may result in ecosystem degradation and, consequently, a loss of tourism revenue. Onshore, the development of new marinas can lead to permanent change to the shoreline [7], and unmanaged mooring can result in littering and vegetation damage [9]. In many areas, leisure boating is the major source of anthropogenic noise and negatively influences animal behavior [10]. Overcrowding on the water also negatively impacts tourists themselves. Tseng et al. [11] revealed that, when boaters saw more people than expected, their sense of safety and the level of enjoyment decreased. In addition to diminishing the quality of the user experience, higher boat densities increase accident risks [12].

It is curious to note that, while it has been recognized as necessary for a long time [13], in many cases, very little data are available regarding the diversity of boating activities in space and time, along with a lack of efficient acquisition methods. This may be due to the fact that monitoring water tourism poses different challenges compared to the (better developed) practice of tracking tourists on land. For example, the physical features of water bodies and the nonlinear character of boating traffic mean that many popular and efficient land monitoring tools, such as eco-counters, cannot be used.

The current techniques for monitoring boating tourism encompass a variety of methods. Data may be collected directly onsite through observations [4,14] and surveys [15,16]. Other indicators—for example, the number of boat launches or mooring places in marinas—have proven to be good proxies of recreational boating activity [3]. However, data capture is time- and labor-consuming, and studies usually have a limited spatial or temporal scope. In this context, statistical [17] and spatial modeling [5] can help to extend empirical results over time and space. The most promising method so far is the analysis of GPS logs [18]. As GPS devices have become widely available, more boats can be followed (although privacy issues associated with tracking must not be neglected [19]). In coastal areas, the Automatic Identification System offers a rich source of data on marine traffic. Designed primarily for safety purposes, it can also be used for boat tracking [20]. However, small recreational craft are not legally required to use the system. Another approach is to collect data using remotely operated cameras [17] or to derive them from aerial and optical SPOT satellite images [5]. However, remote sensing techniques are frequently limited by cloud cover. In this context, the launch of the two Sentinel-1 satellites, which regularly provide dual polarization (VH and VV) radar images independent of weather and light conditions with high spatial resolution, has opened up a new opportunity for recreational boat monitoring.

Radar remote sensing has been widely tested for ship detection at sea, and the literature describes several opportunities and limitations. Ship length and wind speed have been found to have the biggest impact on detection accuracy, along with signal polarization incidence angles [21–23]. It has been reported that the minimum detectable ship length in no wind conditions increases from 7 to 10 m for incidence angles (Θ) 47° and 23°, respectively, for C-band observations [21]. Furthermore, the use of the same incidence angle ($\Theta = 23°$) with RADARSAT HH polarization was found to be more efficient than ERS-1 VV polarization. In another study, Touzi at al. [22] examined fully polarimetric datasets for ship detection. The latter authors confirmed that HH polarization is most effective. Regarding the angle of incidence of observation, in calm sea conditions, the range $\Theta = 20°$ to $\Theta = 60°$ was found to be useful for ship detection; however, as the sea surface roughness increased, observations carried out at incidence angles larger than 55° were not suitable. Regarding Sentinel-1 data, ship detection has been found to become less accurate in wind speeds above 10 m/s [23], especially with VV polarization. The latter study also presented detection results as a function of ship dimensions. For ships shorter than 10 m, recognition was very poor, around 40% for VV polarization and 60% for VH polarization. On the other hand, the detection probability was very good for ships longer than 90 m. An in-depth analysis of the factors that influence ship detectability was given by Tings et al. [24].

The potential use of Synthetic Aperture Radar images for large ship detection has been studied using several different approaches: the wave polarization anisotropy and symmetric scattering characterization method, based on fully polarimetric datasets [22]; the degree of polarization [25]; and the discrete wavelet transform [26]. The most widely-used methods are based on the adaptive threshold or the Constant False Alarm Rate [27–31]. These methods seek to identify pixels with higher values than the value of the local background. Convolutional neural network-based methods have been tested on very high resolution datasets (1–3 m), resulting in accuracies ranging from 68.2 to 88.5% for various network configurations in offshore conditions [32]. Another group of methods uses feature pyramid networks, and boat mapping accuracies range from 88 to 95% [33,34].

Small (10–12 m) and fast boats have been observed using a combination of image processing techniques. Here, the aim is to identify craft by detecting the V-shaped wakes they leave behind [35]. The latter study evaluates the algorithm performance at 93%. Other two-step approaches have been shown to be efficient, but there are significant differences between them. In one study, a convolutional neural network was applied to Gaofen-3 and Sentinel-1 images [36]. In the first step, a self-attention mechanism was used to enhance feature visibility and detection; then, contextual information was used to fine-tune the mapping. Another investigation explored the potential use of polarimetric POLSAR data [37]. The first step was to develop and apply new polarimetric features and suppression manipulation to reduce sea untidiness. In the second step, an enhancement manipulation was applied to highlight the signals from ships.

In this paper, we propose a novel two-step method. Our method uses adaptive thresholding, based on global and local information and math morphology operators, to detect small and slow recreational boats in lake conditions. Although the adaptive thresholding method is widely used for ship detection, it must be modified to adapt it to lake conditions. Notably, we adjust the method used to collect background statistics and add a second step to the algorithm to separate boats merged with the coastline or grouped into multi-objects, etc. To the best of our knowledge, no previous studies have developed a method to map small recreational boats in lake conditions. We also explore the potential use of a boat database, derived from a series of Sentinel-1 images, for the monitoring of recreational ecosystem services.

2. Study Area

2.1. Characteristics of the Study Area

The study area covers the Great Masurian Lakes region in Northeast Poland (Figure 1a). The area is one of the most popular destinations in the country and is visited by over 350,000 tourists each year. One-third of them sail [38], attracted by the many interconnected lakes that allow multi-day trips. The primary route is 110 km long, with numerous secondary waterways. We selected 31 lakes, which form a sailing trail. The area of these lakes varies from 0.34 to 102.14 km^2 (1 lake is larger than 100 km^2, 8 are 10–25 km^2, and 22 are smaller than 10 km^2). All are of glacial origin but have different characteristics; this point is important, as these characteristics can influence boat detection due to wave formation.

- Moraine-dammed lakes are large (minimum distance between shores greater than 1.5 km), with a relatively regular shape. They are mostly surrounded by flat, arable land and meadows. The annual mean wind speed over these lakes varies from 5.49 m/s (the smallest) to 6.06 m/s (the largest). It should also be noted that the mean wind speed is higher in the northern part of the study area. Western winds dominate, followed by southern winds [39].
- Ribbon lakes are very long and narrow. They are surrounded by high banks and forests; the mean wind speed over these lakes varies from 4.44 to 5.45 m/s.
- Kettle lakes are small and round; these lakes are very seldom used for sailing.

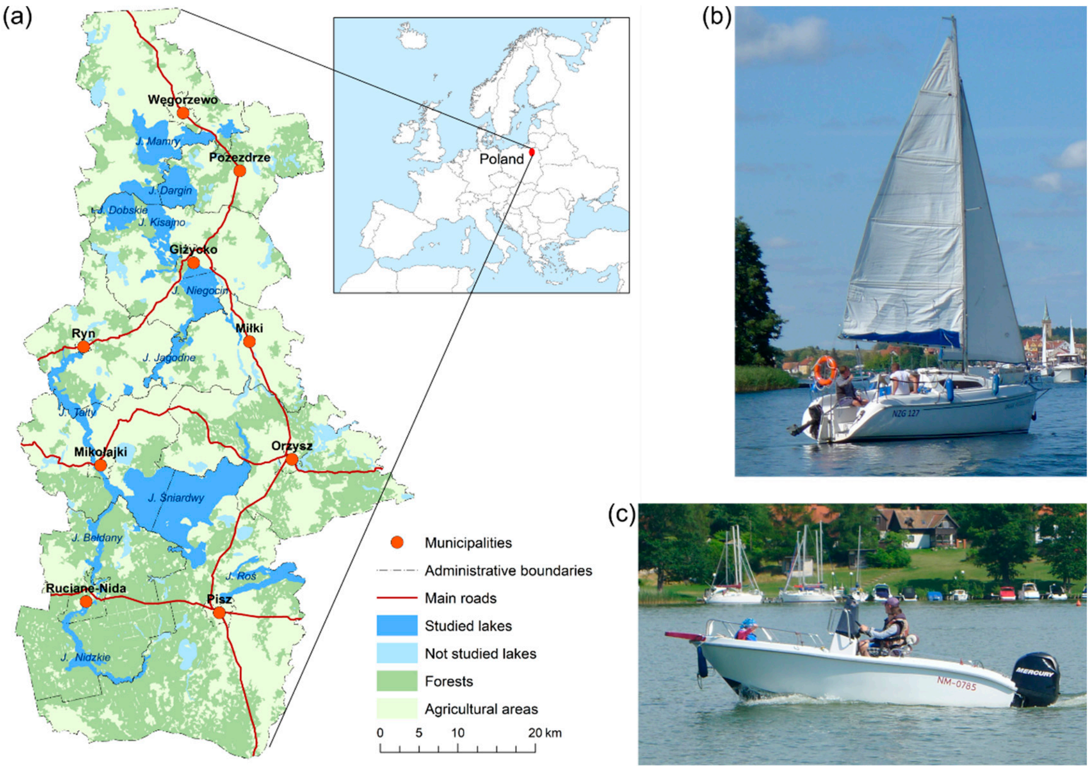

Figure 1. The study area (**a**): typical recreational sailing boat found in the area (**b**) and typical recreational motorboat found in the area (**c**).

2.2. Characteristics of Recreational Boats in the Area

Almost all of the water traffic in the study area is recreational (commercial or industrial ships are rarely found). There are two main types of recreational craft. The most popular are sailing boats (around 91% of all boats), followed by motorboats (9%). Most sailing boats used in the area are relatively small: hull lengths range from 6.36 to 10.7 m; hull widths range from 2.48 to 3.4 m, and the sail areas range from 23 to 55 m^2 (Figure 1b). The standard hull lengths of motorboats range from 5.5 to 12.26 m (Figure 1c). Therefore, the dimensions of these recreational boats are smaller than those reported to be the minimum detectable ship size in sea conditions [21,23].

3. Materials and Methods

3.1. Materials

Our analysis focuses on a set of C-band ground range-detected Sentinel-1 products acquired in dual polarization (VH + VV) mode at 10 m spatial resolution. The sample of images covers seven tourist seasons (15 April–15 October) from 2015 to 2021. Only images captured around 6.15 pm were used as they were the only data available during the day, appropriate for the observation of tourist activities. For the years 2015 and 2016, when only one S-1 satellite operated, around 30 images per season were analyzed; for the other years, around 60 images were selected. To maximize the number of observations, images from different orbits were used. Consequently, it was not always the case that the entire study area was analyzed at the same time, and the number of lake observations per season varied from 9 to 33 for 2015–2016 and 29 to 61 for 2017–2021.

A hydrological map from the Topographic Objects Database (BDOT10k) [40] was used to mask the lakes.

Two types of reference data were used:

- The first consisted of data collected in 2014 and 2015 through structured field observations [14]. All recreational water activities (sailing boats, motorboats, etc.) that took place in viewsheds were described. These observations were used to obtain a model of the spatial distribution of boats [41]. The data derived from field observations can be used for validation at the lake level, as it has a low spatial resolution.

- The second consisted of 769 reference points, collected via a visual interpretation of images captured over seven lakes. These lakes were selected based on their shape (four moraine-dammed lakes and three ribbon lakes) and the intensity of use. Images from 14 dates were randomly selected to cover different weather conditions. Finally, 325 points representing boats, and 444 points representing water were collected (Table 1).

Table 1. Characteristics of the reference datasets.

Lake	Type of Lake	Date	Incident Angle	Wind Speed [m/s]	Number of Reference Points	
					Boats	Water
Bełdany	Ribbon	11/08/2018	38.2–38.5	2	6	43
Bełdany	Ribbon	20/06/2021	38.2–38.5	3	22	25
Dargin	Moraine-dammed	26/04/2019	39.2–39.6	3	13	25
Dargin	Moraine-dammed	19/07/2020	39.2–39.6	1	42	44
Kisajno	Moraine-dammed	05/08/2018	39.1–39.4	1	14	15
Kisajno	Moraine-dammed	13/08/2019	39.1–39.4	3	15	21
Mikołajskie	Ribbon	04/08/2017	38.4–38.6	2	22	25
Mikołajskie	Ribbon	31/07/2020	38.4–38.6	3	10	10
Niegocin	Moraine-dammed	15/08/2015	39.1–39.6	2	42	51
Niegocin	Moraine-dammed	20/07/2021	39.1–39.6	3	22	25
Roś	Ribbon	29/06/2016	39.2–39.8	3	15	17
Roś	Ribbon	16/05/2021	39.2–39.8	4	29	35
Śniardwy	Moraine-dammed	17/07/2017	38.6–39.6	3	6	7
Śniardwy	Moraine-dammed	08/05/2020	38.6–39.6	1	67	101
Sum					325	444

3.2. Method Used to Detect Recreational Boats

We apply a two-step method to detect boats. In the first step, local image statistics are used to extract groups of pixels that are considered to be boat candidates. Next, individual boats are delimited using math morphology operators. The general workflow is shown in Figure 2.

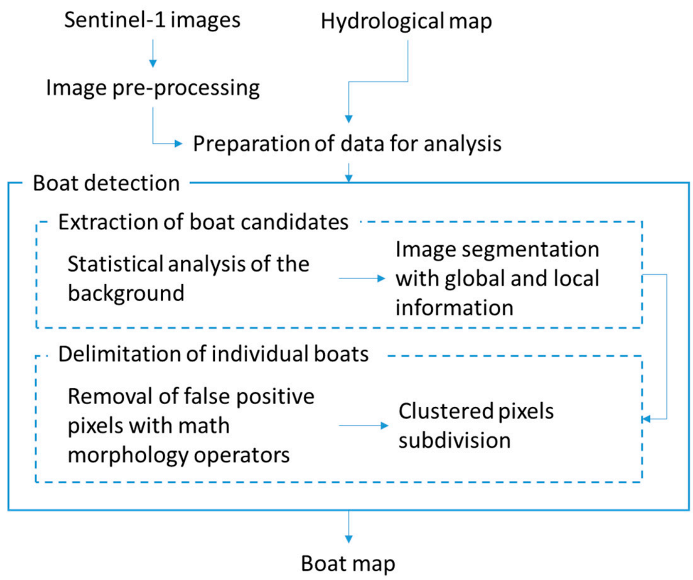

Figure 2. Boat detection workflow.

3.2.1. Image Preprocessing and Data Preparation

All images were downloaded from the CREODIAS image repository. They were then orthorectified and projected onto the UTM 34 system. Incorrect pixels at the edges of the scene were removed.

The algorithm is applied to each lake separately. All satellite images are clipped to a single lake using the hydrological map. Only images that cover the whole area of a specific lake are used in subsequent analyses.

3.2.2. Recreational Boat Detection

Our aim was to detect recreational boats around five times smaller than the area of a Sentinel-1 pixel. While such small craft cannot be detected in sea conditions [23], our goal was to detect recreational boats under calm water (lake) conditions. In particular, we assumed that backscatter (σ_0) from the smooth water surface would be very low and consist mainly of a single specular bounce. At the same time, we expected to find a double bounce at the contact point between the water and a boat, meaning that the signal received by the sensor is significantly stronger (Figure 3).

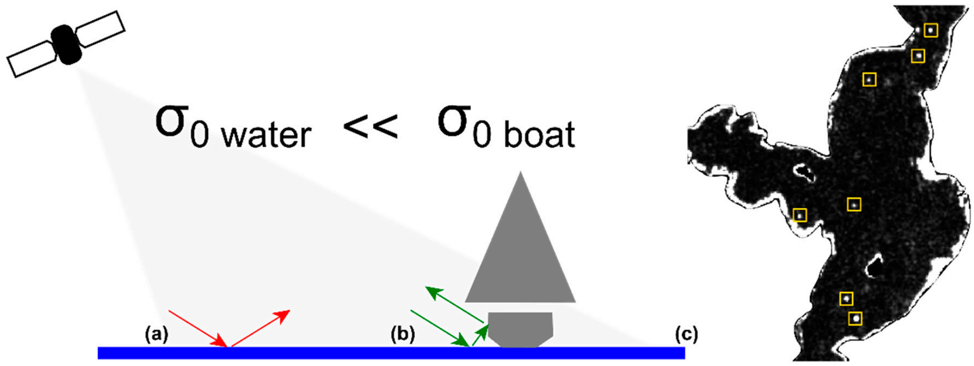

Figure 3. Boat detection method: (**a**) a single specular bounce from the water, (**b**) a double bounce from the boat (σ_0—backscatter), and (**c**) a sample radar satellite image (yellow squares represent boats).

Extraction of boat candidates. VV polarization images were selected for boat detection, as HV images were too noisy (Figure 4). The method searches for pixels with values that are higher than the value of the local background. The local background is usually defined as tiles of different sizes [28,29]. In sea conditions, the optimal size has been established as 200 × 200 pixels [29], which results in an area of 4 km^2. However, this approach is not feasible in lake conditions for the following reasons:

- Lakes are relatively small; the vast majority in our study area are less than 5 km^2.
- Lakes have an irregular shape; hence, the local background, defined as a square tile, may contain multiple pixels that correspond to onshore objects with relatively high backscatter (buildings and forests).
- Recreational boats are small; the power of backscatter received from them is lower than that received from onshore objects.

Consequently, we use the lake surface as the local background. To obtain a clear water area, aquatic vegetation is masked using an internal buffer measuring 50–120 m (depending on the lake). The local background is calculated as the mean ($\bar{x}$) of all pixels containing a clear water area.

Then, based on the entire lake dataset (i.e., not trimmed to the buffer), the standard deviation (σ_w) is calculated in a moving window of a given size. Preliminary tests established that the optimal window size is 11 × 11 pixels. The central pixel in each window is classified as a potential boat location if the following condition is met:

$$\sigma_w > \beta \times \bar{x} \tag{1}$$

where:

σ_w—is the standard deviation calculated in the window of 11 × 11 pixels.

$\bar{x}$—is the mean value of all pixels that contain a clear water area.

β—is a coefficient; this was empirically determined by applying different values and evaluating the results. The optimal value was found to be 0.95.

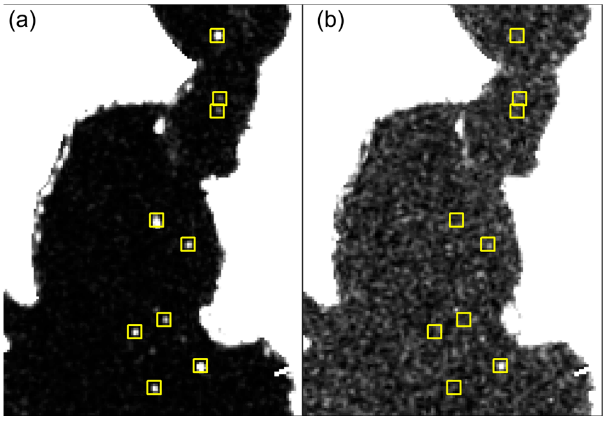

Figure 4. Boat visibility in a Sentinel-1 image (yellow squares represent boats): (**a**) VV polarization and (**b**) VH polarization.

Delimitation of individual boats. The previous step detects candidate boats. However, this dataset contains not only pixels that represent boats but also pixels that represent aquatic vegetation (at the edges of the lake). False positives were identified based on the size of the detected object (10,000 pixels). However, before this condition was applied, it was necessary to distinguish boat detections close to the shore, which were connected to shore pixels. The math morphology operator erosion [42] was applied in a window of 5 × 5 pixels.

Following the removal of clusters of pixels corresponding to the shore and aquatic vegetation, we subdivided boat clusters into individual boats. This was necessary, because boats that are very close to each other can be merged into one object (this happens, for example, during regattas, which are frequently organized during the tourist season). First, the means are calculated for each cluster. Then, only pixels with values higher than the mean are selected. The maximum value recorded for each subdivided object was considered to be a boat.

Finally, annual maps of recreational boat distribution were prepared, and the kernel point density was calculated for all detected objects.

3.2.3. Validation

The results of the classification were validated by:

- checking individual boat detections based on reference points for selected images and the calculation of the error matrix;
- comparing the spatial distribution of all boats detected in 2015 to a distribution model derived from field observations;
- comparing our algorithm's results with results obtained using the object detection algorithm implemented in SNAP software [31].

Checking individual boat detections. For validation purposes, a dilation filter was applied to the final maps of boats. Here, the aim was to compare reference data not only to a boat pixel but also to its close neighborhood. The goal was to avoid small imprecisions due to the collocation of reference points during visual interpretation.

Confusion matrices [43] were calculated separately for each lake and for all reference datasets. The following quality measures were calculated: overall accuracy (OA) and kappa, user's (UA) (commission errors) and producer's (PA) (omission errors) accuracy, and the

F1 score, which is a combination of PA and UA. Additionally, the impact of the second step in the method on the final classification results was checked. Here, we examined the impact of the applied math morphology filters and the multi-object division technique on the method's accuracy.

Checking the spatial distribution of boats. The spatial distribution model calculated from field observations was compared to a boat density map derived from Sentinel-1 satellite images at the lake level. Pearson's correlation coefficient was calculated to measure the linear correlation between these two sets of data.

Comparing our results with results obtained using the object detection algorithm implemented in SNAP software. As our algorithm is based on an adaptive threshold that is similar to the one implemented in SNAP software, we applied the latter to recreational boat detection on images of lakes for which reference datasets were available. Several attempts were made to map the area using various sets of input parameters (different sizes of target, guard, background windows, etc.) in different configurations.

4. Results

4.1. Classification Accuracy

4.1.1. Evaluation of the Boat Detection Method

The overall accuracy obtained for all reference points was 88.17% (kappa 0.76) (Table 2). Commission and omission errors were similar. For boats, PA and UA were equal to 0.86. For water, the errors were slightly lower (PA and UA 0.9). Most omission errors concerned boats situated near to the shoreline. Both omission and commission errors were mostly found in squally areas. In these areas, the surface roughness is notably higher, increasing the local backscatter statistics. Buoys, although very small, were quite often detected as boats. Their typical shape means that they behave as corner reflectors.

Table 2. Recreational boat classification confusion matrix for all reference datasets.

	All Reference Datasets	
	Boat	Water
Boat	281	47
Water	44	397
Producer's accuracy	0.86	0.89
User's accuracy	0.86	0.9
F1 score	0.86	0.9
Overall accuracy	88.17	
Kappa	0.76	

Although during the period of the analysis, the measured wind speed on ribbon lakes was higher than moraine-dammed lakes, they were better classified (OA 91.51 and 86.47, respectively) (Table 3). Moreover, the accuracy did not significantly decrease as the wind speed increased in the case of ribbon lakes. However, this was not the case for moraine-dammed lakes, where a reduction in classification accuracy was clearly visible as the wind speed increased. This finding may be due to wave formation.

Table 3. Recreational boat classification confusion matrix for ribbon and moraine-dammed lakes.

	Ribbon Lakes		**Moraine-Dammed Lakes**	
	Boat	Water	Boat	Water
Boat	90	8	191	39
Water	14	147	30	250
Producer's accuracy	0.87	0.95	0.86	0.87
User's accuracy	0.92	0.91	0.83	0.89
F1 score	0.89	0.93	0.85	0.88
Overall accuracy	91.51		86.47	
Kappa	0.82		0.73	

4.1.2. Evaluation Results as a Function of the Classification Step

Table 4 shows changes in the boat detection accuracy depending on the filter used. In the first step, boat candidate extraction was based on local image statistics. Here, the overall accuracy was 79.71 (kappa 0.58). False positives were found mainly along the shoreline, where areas covered by aquatic vegetation, mainly rushes, were classified as boat candidates. On the other hand, omission errors tended to occur when boat candidates were merged into one object with the shore or other boats.

Table 4. Impact of the application of math morphology filters, and multi-object division techniques on boat detection accuracy.

Erode Filter	Multi-Object Division	Dilation Filter	Producer's Accuracy	User's Accuracy	F1	Overall Accuracy	Kappa
no	no	no	0.74	0.76	0.75	79.71	0.58
no	yes	no	0.78	0.65	0.71	76.00	0.51
yes	no	no	0.72	0.89	0.79	83.78	0.66
yes	yes	no	0.76	0.88	0.81	85.27	0.69
yes	no	yes	0.74	0.91	0.82	85.43	0.70
yes	yes	yes	0.86	0.86	0.86	88.17	0.76

The application of the erode filter and the removal of overly large objects from the classification substantially improved UA (by 0.10–0.15) and reduced commission errors by more than 10%. However, the application of the erode filter alone did not overcome the problem of omission errors. Furthermore, while neither the multi-object division nor dilation steps, applied separately, resolved the problem of omission errors, the application of both reduced the underestimation by 12%. The addition of a second classification step improved the overall boat detection accuracy by 8.5% and the kappa index by 0.18.

4.2. Spatial Distribution of Recreational Boats

At the lake level, the Pearson's correlation coefficient between data derived from field observations and satellite data from Sentiel-1 images was 0.759. However, it should be noted that the dataset derived from satellite images accurately showed the internal diversity of lake use. This information is poorly captured by low spatial resolution field data, especially in large, open lakes where it is impossible to observe the precise location of boats. Figure 5 shows the comparison of the spatial distribution of boats captured with radar and field observations within Śniardwy lake. The general trends are similar, i.e., the western part of the lake is used more intensively. It is due to the close proximity of the neighbouring lakes and the course of the main trail. Both maps show that the rest of the lake is rarely visited by sailors, but in the case of Sentinel-1 based map areas of stone reefs avoided by sailors are seen.

However, in some lakes the differences in spatial distribution of boats are more significant. This is especially seen in Niegocin lake. Although both maps show a high density of boats in the northern part of the lake (see Figure 6), satellite based map indicates a clear concentration close to the entrance to ports, which was not captured by field observation. More important differences are seen in the southern part of the lake. The data derived from Sentinel-1 images shows a very high boat density in the western part, along the sailing trail. It reflects very well natural conditions for sailing, showing clearly unused shallow water areas and the unique safe routes of relatively deep water in that part of the lake. In the case of field study data, the entire southern part of the lake is rarely used. This is related to the limitation of the field study. Several observations were taken from points located close to the ports situated in the northern part of the lake, so remote locations were less visible to the observer. In summary, an analysis of the density of recreational boats based on radar images highlighted the main sailing trails and entrances to the most popular ports. At the same time, zones with very limited traffic were detected. In these cases, access is limited mainly by obstacles such as shallow water or stone reefs.

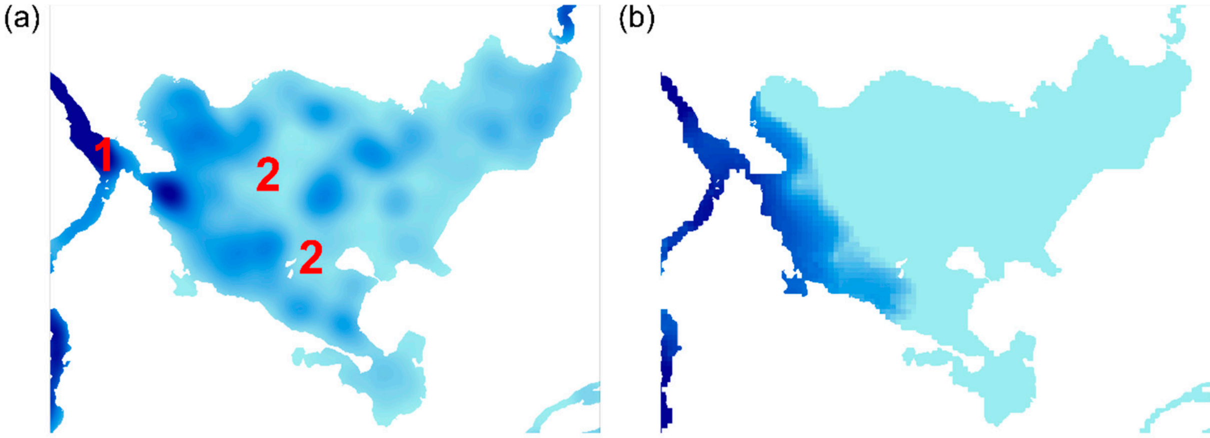

Figure 5. Internal diversity of boat density within Śniardwy lake: (**a**) based on map derived from Sentinel-1 images and (**b**) based on map derived from field observations. 1—main sailing trail, 2— stone reefs.

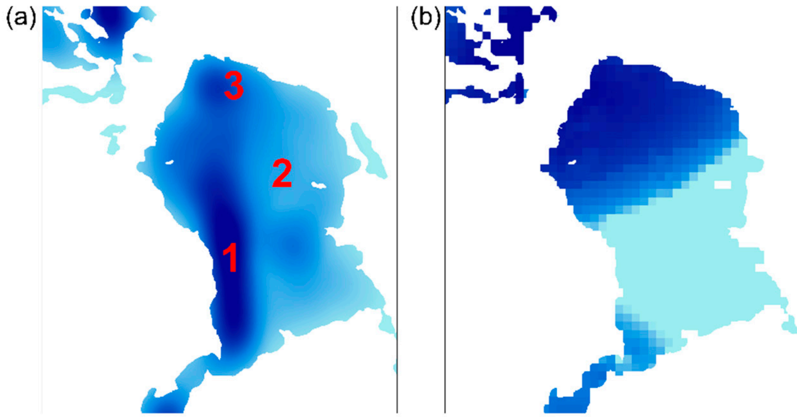

Figure 6. Internal diversity of boat density within Niegocin lake: (**a**) based on map derived from Sentinel-1 images and (**b**) based on map derived from field observations. 1—main sailing trail, 2—shallow water, and 3—entrance to a port (on all the maps).

Regarding the mapping of small recreational boats using the SNAP ship detection algorithm, our analysis demonstrated that, unfortunately, the algorithm did not detect any boats, regardless of the configuration of the input parameters.

Figure 7 shows the spatial distribution of recreational boats within the study area for the period 2015–2021. The figure highlights that the large, interconnected lakes in the northern part of the study area are used much more intensively than the lakes in the south. It is also seen that sailors mainly use the main route, which connects the biggest towns in the area, where the infrastructure is well developed. The analysis showed that large lakes with a high natural potential for sailing but without infrastructure, which are located on secondary waterways, are rarely used.

The spatial patterns of use are similar every year. Table 5 shows a correlation among maps year to year. The results range from 0.47 to 0.73 when comparing the tourist seasons of 2015 and 2016. For those years, the number of images is low because only the Sentinel-1A satellite was operating. The launch of the Sentinel-1B satellite resulted in an increase in the number of observations. It had a significant impact on the correlation among tourist seasons maps from 2017 to 2021, which varies from 0.73 to 0.85. This means that the larger the number of images we have, the more accurate and repeatable the spatial distribution of the boats.

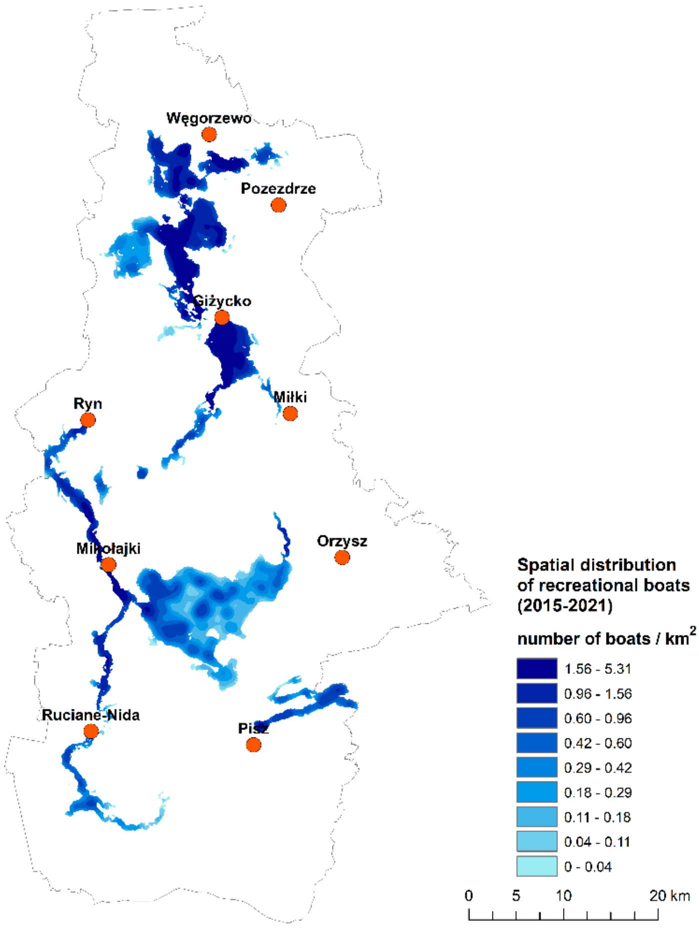

Figure 7. Spatial and temporal distribution of detected recreational boats for the period 2015–2021.

Table 5. A correlation among the spatial distribution of boats.

	2015	2016	2017	2018	2019	2020	2021
2015	1.00	0.47	0.59	0.58	0.47	0.55	0.55
2016		1.00	0.60	0.62	0.54	0.73	0.63
2017			1.00	0.76	0.80	0.84	0.82
2018				1.00	0.67	0.79	0.75
2019					1.00	0.76	0.73
2020						1.00	0.85
2021							1.00

4.3. Temporal Distribution of Recreational Boats

Figure 8 shows the average number of recreational boats per day detected at 6.15 pm in the tourist seasons between 2015 and 2021. The highest peak was in 2019, with 148 recreational boats detected on average per day. The number of boats found in the area increased by about 50% between 2015 and 2019. This shows a great increase of interest in this form of recreation. Surprisingly, the Covid-19 pandemics reversed this trend to a very limited extent. In 2020 we observed only 8 per cent decrease compared to 2019, and in 2021—15 per cent decrease compared to 2020 (Figure 7).

As regular observations were collected during the tourist seasons, it was also possible to establish weekly and monthly recreational use dynamics for each lake. Figure 9a,b present examples of weekly and monthly tourist traffic dynamics for two lakes: Niegocin and Dargin. In both lakes, we can see that most boat users visit the Great Masurian Lakes during the summer season, especially in June, July and August. There are, however, some differences between the lakes: In the case of Niegocin, which is located near the largest town of the region and the main tourist centre, Giżycko, there is a high visitor count per day in August. In the case of Dargin Lake, the visitor movement is much more flat: June, July, and August are frequented almost in the same way. Similar differences occur in weakly patterns: the peak of visitors in Niegocin appears on Saturday and is very visible, while Dargin is visited by a very similar number of boats during a half of the week. This suggests that the spatial-temporal patterns of visitor traffic in both lakes are very different. This, in turn, shows a great advantage of the proposed method. It allows us to monitor visitor movement in a large area in a very precise way. We can compare not only year-to-year changes, but also analyse weekly and monthly patterns at the same time for the same area. No other method can achieve this with such a high degree of spatial accuracy.

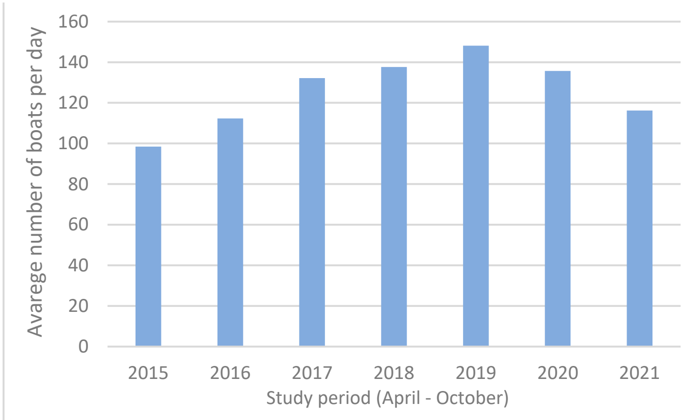

Figure 8. Daily average number of detected recreational boats for the period 2015–2021.

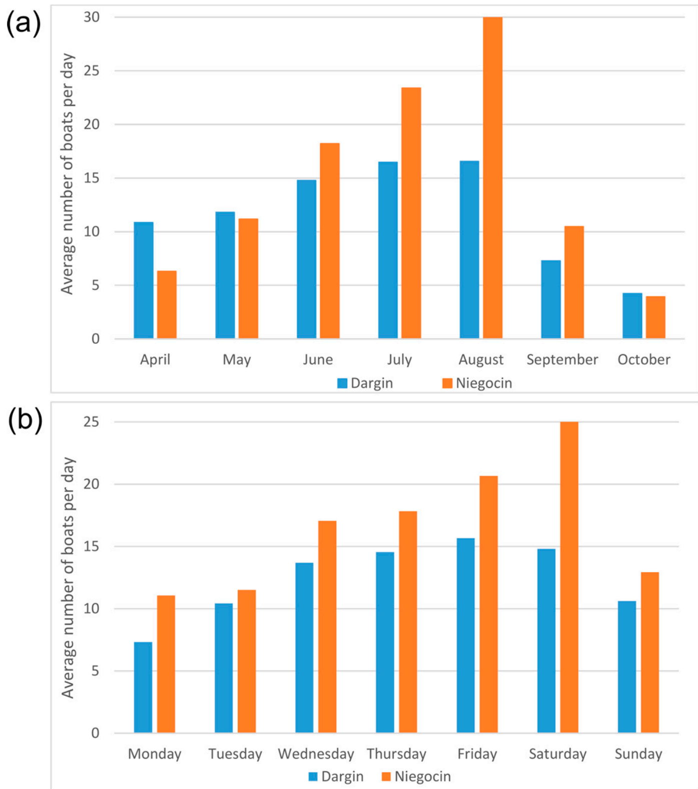

Figure 9. Temporal distribution of detected recreational boats for the period 2015–2021: (**a**) monthly distribution, and (**b**) weekly distribution.

5. Discussion

In this paper, we explored the potential to map small recreational boats using Sentinel-1 data in lake water conditions. Accurate mapping can contribute to monitoring recreational ecosystem services. A great advantage of this method is that it can cover quite a large area at the same time, so it overcomes most of the limitations of traditional methods of monitoring tourism movement, such as time-consuming and labor-consuming field observations or surveys. Moreover, using radar images allows us to apply this method regardless cloud cover, which is problematic for optical remote sensing.

The detection of ships with a hull shorter than 10 m is a known challenge, especially in sea conditions. The detection accuracy is reported to be high (over 90%) for fast-moving ships [35] or low (below 60%) for slow-moving ships [23]. However, our analysis of calm lake water conditions found that the detection rate was higher than 88%, regardless of boat speed. Although we tested our method with recreational boats, it may also be a useful technique to monitor all traffic on inland water bodies.

Previous studies have reported contradictory conclusions regarding the most suitable polarization for ship detection. Pelich et al. [23] found that cross-polarization was more appropriate, while Touzi at al. [22] identified that co-polarization was better. Our study confirms that VV polarization gives more accurate results, while VH polarization is not at all suitable. An incidence angle of around 38° proved to be suitable for small boat detection, which confirms previous observations [22].

The way of collecting the global background value appeared to be crucial for the detection of boat candidates in the image. The previous approach [31], which used square tiles for the statistics collection, was not at all suitable for lake conditions, as they included in the mean calculation multiple pixels that correspond to onshore objects with relatively high backscatter. A more detailed delimitation of the background area made detection possible.

Regarding weather conditions, wind speed has been reported as a factor that can decrease the probability of ship detection [24]. We found that for large moraine-dammed lakes, a higher wind speed reduced the probability of detection, but this was not confirmed for narrow ribbon lakes. Other weather conditions, such as heavy rainfalls, might also influence the results of boat detection, as they increase the roughness of the water surface. However, the images randomly selected for a test sample did not show periods of heavy rain, so it was impossible for us to test it. Future work should explore whether this is a factor that might limit the use of the method.

The presented method proved to be useful for the detection of recreational boats and mapping of their spatial distribution. However, there was one important limitation of this study, which is the exact time of image acquisition. The radar images made for the Great Masurian Lakes were obtained for 6.15 pm, which is not the most optimal time of the day to monitor the recreational ecosystem services. In fact, it may be a significant limitation, especially at the beginning and end of the tourist season, when days are shorter. However, this is not a limitation concerning the method itself, but rather the problem of satellite data availability. Moreover, the correlation between satellite-based maps and field observations proves that this limitation still allows effective use of this method even in this area.

6. Conclusions

The proposed method allowed us to detect small recreational boats in calm (lake) conditions with high accuracy. The use of clear water areas for the calculation of global background statistics was the condition indispensable for detection. The application of math morphology operators improved the accuracy of boat mapping.

The application of the presented method to regularly acquired Sentinel-1 radar data opens up new opportunities for tourism management and infrastructure planning in lake districts. It may also help monitor the environmental impact of water tourism. A test site used in this study proved that the method allows us to examine spatial distribution of tourism traffic on water, and to analyze its temporal patterns: both weakly and seasonal. To the best of our knowledge, no other method of monitoring tourism movement can provide such precise and accurate information on the distribution of recreational boats.

The method developed for the purpose of this study was successfully applied to C-band Sentinel-1 images. Further research can test our method applying it on images acquired with different radar wavelengths (e.g., X-band, L-band) or images of higher spatial resolutions (e.g., ICEYE).

Author Contributions: Conceptualization, E.W., S.K. and M.R.; methodology, M.R. and E.W.; software, M.R.; validation, E.W., M.R., S.K. and M.D.; data curation, M.R. and E.W.; writing—original draft preparation, E.W. and S.K.; writing—review and editing, M.R., S.K., M.D. and E.W.; visualization, M.R. and E.W.; supervision, E.W. and S.K.; and funding acquisition, S.K. and E.W. All authors have read and agreed to the published version of the manuscript.

Funding: This study was carried out within the framework of European Union's Horizon 2020 research and innovation program under grant agreement no. 952111, entitled 'Earth Observation Training in Science and Technology at the Space Research Centre of the Polish Academy of Sciences—EOTiST'. The field data collection was supported by the Narodowe Centrum Nauki, Poland, under grant no. DEC-2012/07/B/HS4/00306, entitled 'The use of ecosystem services concept for the sustainable tourism management—an example of lake areas'.

Data Availability Statement: Not applicable.

Conflicts of Interest: The authors declare no conflict of interest.

References

1. Hall, C.M.; Härkönen, T. (Eds.) *Lake Tourism: An Integrated Approach to Lacustrine Tourism Systems*; Channel View Publications: Clevedon, UK, 2006; Volume 32, 235p.
2. Hall, C.M. Trends in ocean and coastal tourism: The end of the last frontier? *Ocean Coast. Manag.* **2001**, *44*, 601–618. [CrossRef]
3. McCole, D.; Joppe, M. The search for meaningful tourism indicators: The case of the international upper great lakes study. *J. Policy Res. Tour. Leis. Events* **2014**, *6*, 248–263. [CrossRef]
4. Venturini, S.; Massa, F.; Castellano, M.; Fanciulli, G.; Povero, P. Recreational boating in the Portofino Marine Protected Area (MPA), Italy: Characterization and analysis in the last decade (2006–2016) and some considerations on management. *Mar. Policy* **2021**, *127*, 103178. [CrossRef]
5. Landré, M. Analyzing yachting patterns in the Biesbosch National Park using GIS technology. *Technovation* **2009**, *29*, 602–610. [CrossRef]
6. Leon, L.M.; Warnken, J. Copper and sewage inputs from recreational vessels at popular anchor sites in a semi-enclosed Bay (Qld, Australia): Estimates of potential annual loads. *Mar. Pollut. Bull.* **2008**, *57*, 838–845. [CrossRef]
7. Hansen, J.P.; Sundblad, G.; Bergström, U.; Austin, Å.N.; Donadi, S.; Eriksson, B.K.; Eklöf, J.S. Recreational boating degrades vegetation important for fish recruitment. *Ambio* **2019**, *48*, 539–551. [CrossRef]
8. Balaguer, P.; Diedrich, A.; Sardá, R.; Fuster, M.; Cañellas, B.; Tintoré, J. Spatial analysis of recreational boating as a first key step for marine spatial planning in Mallorca (Balearic Islands, Spain). *Ocean. Coast. Manag.* **2011**, *54*, 241–249. [CrossRef]
9. Skłodowski, J.; Sater, J.; Strzyżewski, T. Presja turystyki wodnej w ekotonach leśno− jeziornych na przykładzie jeziora Bełdany. *Sylwan* **2006**, *10*, 65–71.
10. Rako, N.; Fortuna, C.M.; Holcer, D.; Mackelworth, P.; Nimak-Wood, M.; Pleslić, G.; Picciulin, M. Leisure boating noise as a trigger for the displacement of the bottlenose dolphins of the Cres–Lošinj archipelago (northern Adriatic Sea, Croatia). *Mar. Pollut. Bull.* **2013**, *68*, 77–84. [CrossRef]
11. Tseng, Y.P.; Kyle, G.T.; Shafer, C.S.; Graefe, A.R.; Bradle, T.A.; Schuett, M.A. Exploring the Crowding–Satisfaction Relationship in Recreational Boating. *Environ. Manag.* **2009**, *43*, 496–507. [CrossRef]
12. Riungu, G.K.; Hallo, J.C.; Backman, K.F.; Brownlee, M.; Beeco, J.A.; Larson, L.R. Water-based recreation management: A normative approach to reviewing boating thresholds. *Lake Reserv. Manag.* **2020**, *36*, 139–154. [CrossRef]
13. Ashton, P.G.; Chubb, M. A preliminary study for evaluating the capacity of waters for recreational boating 1. *JAWRA J. Am. Water Resour. Assoc.* **1972**, *8*, 571–577. [CrossRef]
14. Kulczyk, S.; Woźniak, E.; Derek, M.; Kowalczyk, M. Pomiar marszrutowy jako narzędzie monitoringu aktywności turystycznej. Przykład Wielkich Jezior Mazurskich. *Probl. Ekol. Kraj.* **2015**, *29*, 111–120.
15. Ryan, K.L.; Hall, N.G.; Lai, E.K.; Smallwood, C.B.; Tate, A.; Taylor, S.M.; Wise, B.S. Statewide Survey of Boat-Based Recreational Fishing in Western Australia 2017/18. 2019. Available online: https://www.fish.wa.gov.au/Documents/research_reports/frr297.pdf (accessed on 2 March 2023).
16. Gray, D.L.; Canessa, R.; Rollins, R.; Keller, C.P.; Dearden, P. Incorporating recreational users into marine protected area planning: A study of recreational boating in British Columbia, Canada. *Environ. Manag.* **2010**, *46*, 167–180. [CrossRef]

17. Afrifa-Yamoah, E.; Taylor, S.M.; Mueller, U. Modelling climatic and temporal influences on boating traffic with relevance to digital camera monitoring of recreational fisheries. *Ocean. Coast. Manag.* **2021**, *215*, 105947. [CrossRef]
18. Pelot, R.; Wu, Y. Classification of recreational boat types based on trajectory patterns. *Pattern Recognit. Lett.* **2007**, *28*, 1987–1994. [CrossRef]
19. Van den Bemt, V.; Doornbos, J.; Meijering, L.B.; Plegt, M.; Theunissen, N. Teaching ethics when working with geocoded data: A novel experiential learning approach. *J. Geogr. High. Educ.* **2018**, *42*, 293–310. [CrossRef]
20. Meijles, E.W.; Daams, M.N.; Ens, B.J.; Heslinga, J.H.; Sijtsma, F.J. Tracked to protect-Spatiotemporal dynamics of recreational boating in sensitive marine natural areas. *Appl. Geogr.* **2021**, *130*, 102441. [CrossRef]
21. Vachon, P.W.; Campbell, J.W.M.; Bjerkelund, C.A.; Dobson, F.W.; Rey, M.T. Ship Detection by the RADARSAT SAR: Validation of Detection Model Predictions. *Can. J. Remote Sens.* **1997**, *23*, 48–59. [CrossRef]
22. Touzi, R.; Charbonneau, F.J.; Hawkins, R.K.; Vachon, P.W. Ship detection and characterization using polarimetric SAR. *Can. J. Remote Sens.* **2004**, *30*, 552–559. [CrossRef]
23. Pelich, R.; Longépé, N.; Hajduch, G.; Mercier, G. Performance evaluation of Sentinel-1 data in SAR ship detection. In Proceedings of the IEEE International Geoscience and Remote Sensing Symposium (IGARSS), Milan, Italy, 26–31 July 2015.
24. Tings, B.; Bentes, C.; Velotto, D.; Voinov, S. Modelling ship detectability depending on TerraSAR-X-derived metocean parameters. *CEAS Space J.* **2019**, *11*, 81–94. [CrossRef]
25. Shirvany, R.; Tourneret, J.Y. Ship and Oil-Spill Detection Using the Degree of Polarization in Linear and Hybrid/Compact Dual-Pol SAR. *IEEE J. Sel. Top. Appl. Earth Obs. Remote Sens.* **2012**, *5*, 885–892. [CrossRef]
26. Trello, M.; Lopez-Martinez, C.; Mallorqui, J.J. A Novel Algorithm for Ship Detection in SAR Imagery Based on the Wavelet Transform. *IEEE Geosci. Remote Sens. Lett.* **2005**, *2*, 201–205. [CrossRef]
27. Robey, F.C.; Fuhrmann, D.R.; Kelly, E.J.; Nitzberg, R. A Cfar Adaptive Matched-Filter Detector. *IEEE Trans. Aerosp. Electron. Syst.* **1992**, *28*, 208–216. [CrossRef]
28. Gao, G. A Parzen-Window-Kernel-Based CFAR algorithm for ship detection in SAR Images. *IEEE Geosci.Remote Sens. Lett.* **2011**, *8*, 557–561. [CrossRef]
29. Greidanus, H.; Alvarez, M.; Santamaria, C.; Thoorens, F.X. The SUMO Ship Detector Algorithm for Satellite Radar Images. *Remote Sens.* **2017**, *9*, 246. [CrossRef]
30. Gao, G.; Gao, S.; He, J.; Li, G. Adaptive Ship Detection in Hybrid-Polarimetric SAR Images Based on the Power-Entropy Decomposition. *IEEE Trans. Geosci. Remote Sens.* **2018**, *56*, 5394–5407. [CrossRef]
31. Crisp, D.J. *The State-of-the-Art in Ship Detection in Synthetic Apreture Radar Imagery*; DSTO-RR-0272; Defence Science and Technology Organisation Salisbury (Australia) Info Sciences Lab.: Edinburgh, Australia, 2004.
32. Wei, S.; Zeng, X.; Qu, Q.; Wang, M.; Su, H.; Shi, J. HRSID: A High-Resolution SAR Images Dataset for Ship Detection and Instance Segmentation. *IEEE Access* **2020**, *8*, 120234–120254. [CrossRef]
33. Zhang, T.; Zhang, X.; Ke, X. Quad-FPN: A Novel Quad Feature Pyramid Network for SAR Ship Detection. *Remote Sens.* **2021**, *13*, 2771. [CrossRef]
34. Sun, Z.; Meng, C.; Cheng, J.; Zhang, Z.; Chang, S. A Multi-Scale Feature Pyramid Network for Detection and Instance Segmentation of Marine Ships in SAR Images. *Remote Sens.* **2022**, *14*, 6312. [CrossRef]
35. Grosso, E.; Guida, R. A New Automated Ship Wake Detector for Small and Go-Fast Ships in Sentinel-1 Imagery. *Remote Sens.* **2022**, *14*, 6223. [CrossRef]
36. Wang, C.; Su, W.; Gu, H. Two-stage ship detection in synthetic aperture radar images based on attention mechanism and extended pooling. *J. Appl. Remote Sens.* **2020**, *14*, 044522. [CrossRef]
37. Zhang, T.; Quan, S.; Yang, Z.; Guo, W.; Zhang, Z.; Gan, H. A Two-Stage Method for Ship Detection Using PolSAR Image. *IEEE Trans. Geosci. Remote Sens.* **2022**, *60*, 5236918. [CrossRef]
38. Kulczyk, S.; Derek, M.; Woźniak, E. Zagospodarowanie turystyczne strefy brzegowej jezior na potrzeby żeglarstwa-przykład wielkich jezior mazurskich. *Prace Studia Geogr.* **2016**, *61*, 27–49.
39. Available online: https://globalwindatlas.info/en/ (accessed on 1 November 2022).
40. Available online: https://www.geoportal.gov.pl/dane/baza-danych-obiektow-topograficznych-bdot (accessed on 1 November 2022).
41. Kulczyk, S.; Woźniak, E.; Derek, M. Landscape, facilities and visitors: An integrated model of Recreational Ecosystem Services. *Ecosyst. Serv.* **2018**, *31*, 491–501. [CrossRef]
42. Serra, J. Introduction to mathematical morphology. *Comput. Vis. Graph. Image Process.* **1986**, *35*, 283–300. [CrossRef]
43. Congalton, R.G. A Review of Assessing the Accuracy of Classifications of Remotely Sensed Data. *Remote Sens. Environ.* **1991**, *37*, 35–46. [CrossRef]